HHS Public Access

Author manuscript

ACS Synth Biol. Author manuscript; available in PMC 2022 August 20.

Published in final edited form as:

ACS Synth Biol. 2021 August 20; 10(8): 2076–2086. doi:10.1021/acssynbio.1c00245.

Exploring the tunability and dynamic properties of MarR-PmarO sensor system in *Escherichia coli*

Yusong Zou[1,a], **Chenyi Li**[1,a], **Ruihua Zhang**[1], **Tian Jiang**[1], **Ning Liu**[2], **Jian Wang**[1], **Xianqiao Wang**[2], **Yajun Yan**[1,*]

[1]School of Chemical, Materials and Biomedical Engineering, College of Engineering, The University of Georgia, Athens, GA, 30602, USA

[2]School of Environmental, Civil, Agricultural, and Mechanical Engineering, College of Engineering, The University of Georgia, Athens, GA, 30602, USA

Abstract

Transcriptional factor-based biosensors (TFBs) have been widely used in dynamic pathway control or high-throughput screening. Here, we systematically explored the tunability of a salicylic acid responsive regulator MarR from *Escherichia coli* aiming to explore its engineering potential. The effect of endogenous MarR in *E. coli* on the MarR-PmarO biosensor system was investigated. Furthermore, to investigate the function of marO binding boxes in this biosensor system, a series of hybrid promoters were constructed by placing the marO binding boxes in the strong constitutive pL promoter. The engineered hybrid promoters became responsive to MarR and salicylic acid. To further study the influence of each nucleotide in the marO box on MarR binding, we employed dynamic modeling to simulate the interaction and binding energy between each nucleotide in the marO boxes with the corresponding residues on MarR. Guided on the results of simulation, we introduced mutations to key positions on the hybrid promoters and investigated corresponding dynamic performance. Two promoter variants I12AII4T and I12AII14T that exhibited improved responsive strengths and shifted dynamic ranges were obtained, which can be beneficial for future metabolic engineering research.

Graphical Abstract

*Correspondence: yajunyan@uga.edu.

[a]Yusong Zou and Chenyi Li contributed equally to this work

Author contribution

Y.Z., C.L., and Y.Y. conceived this study. Y.Z. performed the experiments. C.L. and Y.Z. wrote the manuscript. N.L., X.W., and R.Z. assisted in dynamic modeling. C.L., T.J., J.W., and Y.Y. revised the manuscript. Y.Y. directed the research.

Conflict of Interest statement

The authors declare no competing financial interest.

Supporting Information

Additional experimental details and data, including the toxicity of SA on *E. coli*, the test of whether MarR can regulate pL promoter, the test of whether the SA toxicity would cause decreased protein expression, the simulation results of binding frequencies of MarR-DNA complex, and the test of whether enhanced MarR expression affects the performance of promoter variants.

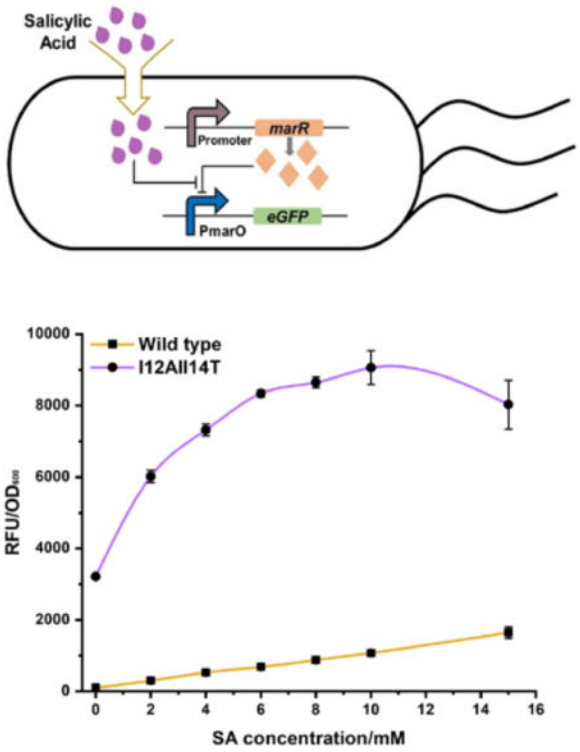

The upper part of the abstract graphic is the schematic graph of MarR-PmarO biosensor system. MarR protein binds on PmarO to inhibit promoter expression, after feeding salicylic acid, this repression can be released. The bottom half of the abstract graphic is the dynamic performance of wild type and variant I12AII14T, which positively shifted dynamic range and enhanced the responsive strength of the promoter towards SA.

Keywords

MarR; transcriptional factor; biosensor; salicylic acid; dynamic regulation

Introduction

In the past decades, metabolic engineering has been demonstrated as a promising approach for developing sustainable bioeconomy [1-3]. Both engineered native and synthetic pathways have been utilized to produce various compounds such as renewable feedstocks [4], biofuels [5], pharmaceuticals [6] and bulk chemicals [7-8]. Current engineering efforts are mostly committed to improve efficiency of pathways performance for high titers, yields and productivities. To this end, rational and random engineering approaches have been widely used. While rational strain engineering is limited by the high physiological complexity of microbes, random mutagenesis strategies are restricted by the selection and screening capacity, which requires reliable tools to monitor product formation [9]. To address these problems, transcriptional factor-based biosensors (TFBs) have been extensively applied in high-throughput screening in recent years [2, 10-11]. TFBs tune the gene expression based on the interaction between ligand and regulator [12]. Coupling TFBs with colorimetric or growth-essential reporter genes

could effectively increase the efficiency of high-throughput screening, and this has been successfully demonstrated in the improvement of mevalonate [13], L-lysine [14], and triacetic acid lactone [15] production. TFBs have also been proven important in metabolic engineering efforts through dynamic regulation of metabolic flux as exemplified in the improvement of lycopene productions [16], layered dynamic regulation of glucaric acid production [17], the regulation of fatty acid synthesis by FadR [18-19] and enhancement in the synthesis of muconic acid by catR [20]. However, despite the advancements and progress made so far, leaky expression and narrow dynamic range remain obstacles for broader applications of TFBs [2]. Thus, research efforts are required to establish efficient workflows for exploring and optimizing TFBs to enhance their applicability.

The multiple antibiotic resistance regulator (MarR) from *Escherichia coli* was first identified by Cohen and coworkers [21]. This regulator recognizes two marO binding boxes located in the promoter PmarO of the MarRAB operon. The expression of the MarRAB operon is repressed in the presence of MarR, but salicylic acid (SA) was found to dissociate the binding between MarR and PmarO and release such inhibition [22]. This SA-mediated dissociation was also confirmed by an *in vitro* test with varied concentration of SA [23]. In the referred study, the addition of 2mM SA was able to dissociate the binding between MarR and PmarO promoter [23]. To further explore the mechanism of MarR, the crystal structure of MarR was resolved [24], and a helix-turn-helix structure contributing to the DNA binding of MarR was characterized [25]. With such knowledge, Zhang and coworkers attempted to engineer this MarR-based system by placing the binding boxes on different promoter regions and reported the corresponding dynamic ranges [18]. However, only four promoters were tested in this work, and the dynamic properties of the MarR and PmarO biosensor system were not further explored. Notably, a recent finding demonstrated a different mechanism for MarR biosensor which employs copper as the signal, and SA could serve as an indirect effector to induce this sensor system [26]. Although the structure and binding mechanism of the MarR-based regulator have been studied extensively, the usability for this sensor has not been thoroughly tested. Thus, to expand the applicability of this biosensor, further understanding of its engineering potential is needed.

In this work, we systematically studied the tunability of MarR-PmarO biosensor system to explore its engineering potential. First, as MarR natively exist in the *E. coli*'s genome, the dynamic range of the biosensor system in both wild type *E. coli* and *E. coli* Δ*marR* were characterized. The promoter PmarO can reach a 2.36-fold increase in activity when the endogenous MarR was deleted. The fine-tuning of MarR expression levels also resulted in a 1.90-fold increase in the responsive strength induced by 15mM SA. To understand the function of the marO binding boxes located in the PmarO promoter region, we constructed a series of hybrid promoters and demonstrated these boxes can function in a "plug-and-play" manner. To better understand the behavior of this biosensor, we employed molecular models to simulate the DNA binding process of MarR. The modeling results revealed several critical nucleotides in each binding box. These nucleotides were predicted to dominate the interaction with MarR. Based on the results of model simulation, we selected these nucleotides as site-directed mutagenesis targets in order to weaken the binding energy between marO binding box and MarR protein. Eventually, two promoter variants, the I12AII4T and II12AII14T, were obtained, which can enable positively shifted dynamic

ranges and enhanced responsive strengths. In summary, we systematically investigated the tunability and engineering potentials of MarR-PmarO biosensor system. The optimized biosensor can be readily applied in high-throughput screening and dynamic pathway regulations on the biosynthesis of SA and derived products.

Results

Re-establishment and validation of MarR-PmarO biosensor system

Salicylic Acid (SA) is an important precursor for many high-value aromatic compounds and an SA responsive biosensor system MarR-PmarO would benefit the dynamic regulation of SA derived synthesis and high-throughput screening of productive candidates for SA and SA derivatives. To examine the applicability of the MarR-PmarO sensor system, we first re-established the sensor system in *E. coli* BW25113 (F') strain by using a two-plasmid configuration (Figure 1a). The PmarO promoter was used to control the expression of a green fluorescence reporter gene eGFP in a high-copy number plasmid pZE12-luc, resulting in pZE12-PmarO-eGFP. The MarR protein was under the control of a constitutive promoter lpp1.0 in a medium-copy number plasmid pCS27 [27-28], resulting in pCS27-lpp1.0-marR. The promoter activity of PmarO was reflected by the fluorescence intensity normalized by OD_{600}. As the positive control (PC), the fluorescence intensity of the strain harboring only the pZE12-PmarO-eGFP was measured, with a normalized intensity of 4570±92 a.u. can be achieved (Figure 1b). When further introducing the pCS27-lpp1.0-marR into wild type *E. coli* BW25113 (F') strain, the intensity was reduced to 253±4.9 a.u. (Figure 1b), indicating that MarR can inhibit the promoter PmarO. Then, gradient concentrations of SA (2mM, 4mM, 6mM, 8mM, 10mM, and 15mM) were added into the medium to induce the biosensor system. The maximum concentration for induction was set to 15mM due to the toxicity of SA (Supplementary Figure S1). The constructed MarR-PmarO biosensor system in *E. coli* strain could respond up to 15mM SA and the fluorescence intensity was from 253±4.9 to 1514±186 a.u. (Figure 1b). These results demonstrated that our re-constructed MarR-PmarO biosensor system was functional and could be activated by SA, which was consistent with previous studies [18, 22-23]. However, we noticed that SA could only partially release repression (33.13%) of wild type MarR-PmarO biosensor system. Thus, further engineering efforts need to be taken to improve the low output strength of this sensor system.

Investigate the effect of the endogenous MarR on MarR-PmarO biosensor system

Since the regulator MarR natively exists in *E. coli* BW25113 (F') strain, we hypothesized that the endogenous MarR might affect the performance of MarR-PmarO biosensor system when the biosensor system was tested in wild-type *E. coli* strain. To test this possibility, the endogenous *marR* gene was knocked out from wild type *E. coli* BW25113 (F') by homologous recombination. Again, as a positive control, the fluorescent intensity of the knockout strain harboring only the pZE12-PmarO-eGFP was tested to be 10787±533 a.u. This represented a 2.36-fold increase in eGFP expression compared to that in the wild type *E. coli* strain (4570±92 a.u.) (Figure 1b), which indicated that the endogenous MarR also exhibited an apparent inhibition effect on PmarO promoter. Observing this, we wanted to further investigate the effect of endogenous MarR on the dynamic performance

of MarR-PmarO biosensor system. Thus, two plasmids pZE12-PmarO-eGFP and pCS27-plpp1.0-marR were introduced into the strain *E. coli* Δ*marR*. While SA could still dissociate the MarR-DNA binding and activate PmarO, the induced promoter strength by 15mM SA in the knockout strain was only slightly higher (8.7%) than that in wild type *E. coli*, indicating that the endogenous MarR only showed limited influence on the dynamic performance when exogenous MarR was introduced. This was likely because the expression level of MarR from the plasmid was much higher than the endogenous copy in genome. Although the dynamic range in knockout strain showed a slight increase compared with wild type, the strength of PmarO induced by 15mM SA can only be recovered by 15.25%, with a fluorescence intensity of 1646±161 a.u. In this circumstance, the limited dynamic range can be a bottleneck for applying this biosensor system in metabolic engineering, and the excessive amount of MarR expressed from plasmid was likely to be the reason for the narrow dynamic range. Therefore, we next sought to fine-tune the MarR expression levels to extend dynamic range. In order to get a clean background, the strain *E. coli* Δ*marR* was used in our following experiments.

Fine-tuning MarR expression level to optimize MarR-PmarO biosensor system

We hypothesized that the excessive MarR protein might be the reason for the limited dynamic range. To test this hypothesis, a previous constructed lpp promoter library containing lpp promoter variants with different strengths was adopted to change the expression level of exogenous MarR [28]. Aiming to weaken the interaction between MarR and the PmarO promoter, lpp promoter variants with decreased strengths, including lpp0.8, lpp0.5, lpp0.2, lpp0.03 (the number behind lpp indicates the relative strength to wild type lpp1.0 promoter), were chosen as candidates. Substituting lpp1.0 with lpp0.2 or lpp0.03 caused evident leaking expression on the sensor system even without introducing SA in *E. coli* Δ*marR*, with the eGFP expression levels reaching over 7000 a.u. (Figure 1c) Nonetheless, the sensor system can still respond to the SA and exhibited increased expression levels of eGFP (Figure 1c). The highest induced strengths of PmarO promoter with lpp0.2 and lpp0.03 controlled MarR were 12468±286 and 12755±1102 a.u. after feeding 5mM SA, respectively (Figure 1c). Further increase of SA concentrations failed to improve the output strength of PmarO (Figure 1c), which was likely due to the toxicity of SA. While substituting lpp1.0 with lpp0.8 did not result in evident influence on the dynamic range, the substitution with lpp0.5 enabled an increased response of MarR-PmarO sensor system towards SA at all tested concentrations (Figure 1c). When induced by 15mM SA, the output strength of the sensor system (2053±134 a.u.) showed a 1.90-fold increase compared to when MarR was controlled by lpp1.0 (1079±55 a.u.), and no obvious leaky expression can be observed when no SA was added (Figure 1c). These results demonstrated that a decreased expression level of MarR can improve the dynamic range, but insufficient MarR availability can result in evident leaky activity of PmarO.

Exploring the function of marO boxes by constructing hybrid promoters

There are two previously identified marO binding boxes in the PmarO promoter, one overlapped with the −10 region of PmarO and the other one located after the −10 region [21-22] (Figure 2a). We hypothesized that the marO binding boxes can function in a “plug-and-play” manner. Thus, placing the binding boxes in a constitutive promoter would

convert it to a MarR-controllable promoter. To test this hypothesis, we chose the strong constitutive promoter pL as the target because pL promoter and its derivatives are widely used in synthetic biology [29-30]. Also, the pL promoter cannot be controlled by MarR (Supplementary Figure S2a). In the natural MarRAB operon, the MarR binds to the marO binding boxes and blocks the access of RNA polymerase to the −10 region in promoter, which hinders the transcription of the downstream genes [21-23]. Based on this mechanism, the marO binding boxes need to be placed on the positions that are near or overlap with the −35 or −10 region to hamper the binding of RNA polymerase. Thus, a total of five sites in the pL promoter were selected for placing marO binding boxes on these sites. The five sites are located before −35 region (site 1), overlapping with −35 region (site 2), located between the −35 and −10 region (site 3), overlapping with −10 region (site 4), and located behind the −10 region (site 5), respectively (Figure 2a, see Methods for detailed locations of each site). We decided to first insert just one box to each site to test the feasibility of creating MarR-controllable hybrid promoters. Based on previous studies, binding box I and binding box II can be recognized by MarR individually, but binding box I enabled a higher repression level, which demonstrated that binding box I was dominant in MarR binding [31]. Thus, the binding box I was placed on these five sites individually to substitute the original pL promoter sequence, resulting in hybrid promoters S1 to S5. As a positive control, the eGFP expression level in strain *E. coli* Δ*marR* under the control of hybrid promoters S1~S5 were determined. The promoter S1, S3, and S4 enabled fluorescent intensities over 7000 a,u, showing promoter strengths close to the PmarO (WT), while only 1628±41 a.u and 2701±502 a.u can be achieved by S2 and S5, respectively (Figure 2b). Next, we further introduced pCS27-lpp0.5-marR into strain *E. coli* Δ*marR* to explore their dynamic performance. Upon the introduction of MarR, all five promoters exhibited a decreased expression level of eGFP, indicating that the MarR was able to suppress the hybrid promoters. A concentration of 10mM SA was used to induce the hybrid promoters. Unexpectedly, only very slight increase can be observed in all five promoters induced by SA, with the highest increase showing in promoter S5 (from 1466±4 to 1680±40 a.u.) (Figure 2b). These results indicated that MarR can inhibit the promoter with only one binding box, but this inhibition was only slightly released by SA. The reason for failing to activate the hybrid promoters when only one binding box was placed in the promoter region was unclear, but similar results were also observed in previous studies for AraC and LuxR when only one operator sequence was added to the core and proximal regions (the location of site 2 to site 5 in this study) [32-34].

We hypothesized that the insufficient activation by SA was due to the lack of a second binding box, as there are two binding boxes in the PmarO promoter in the natural MarR-PmarO sensor system. Therefore, to test this hypothesis, a series of dual-site hybrid promoters were designed and constructed. Appropriate intervals between two binding boxes need to be reserved when placing two binding boxes to the promoter, so only six hybrid promoters were constructed (see Methods for details), namely the S13, S14, S15, S24, S25, and S35 (the numbers indicate the sites used to place the binding boxes). Again, as a positive control, the fluorescent intensities of eGFP enabled by each dual-site hybrid promoters were determined. The highest eGFP expression level was achieved by promoter S15 (9895±1848 a.u.), closely followed by S14 (9662±1368 a.u.), while the S25, S13, S24, and S35 can

only enable fluorescent intensities of 5720±734, 5656±295, 4001±177, and 2249±126 a.u., respectively (Figure 2c). To check whether the dual-site promoters can be regulated by MarR and activated by SA, the pCS27-lpp0.5-MarR was further introduced into *E. coli* Δ*marR* strain along with the hybrid promoters, and 10mM SA was added to induce all six dual-site promoters. Upon the introduction of MarR, all six dual-site hybrid promoters exhibited decreased promoter activities when no SA was present, but the promoter S24 and S25 showed evident leaky activities. Only 32.61% activity of S24 and 51.74% activity of S25 can be repressed by MarR (Figure 2c). For S13 and S15, although these two promoters can be effectively inhibited by MarR (with over 97% activity of the promoter can be repressed), there were only neglectable increases in eGFP expression level that can be observed when 10mM SA was present (Figure 2c). These results indicated that these two promoters still cannot be activated by the SA. As for the promoter S24 and S25 which showed obvious leaky activity when MarR was introduced, they can be effectively induced with 10mM SA, with the 100% activity of S24 and 76.12% activity of S25 can be recovered at this concentration (Figure 2c). These two promoters with medium promoter strengths and excellent inducibility by SA might be helpful in future dynamic regulation of SA related biosynthesis. The promoter S35, which showed the lowest fully induced activity among six dual-site promoters, can recover 44.84% activity after induced by SA. The best performer was the promoter S14. The non-repressed promoter strength of S14 was comparable to the PmarO (WT). It also exhibited a higher promoter activity (1647±58 a.u.) than that of WT (1075±92 a.u.) when induced by 10mM SA. Observing this, we further tested the dynamic range of the MarR-S14 system and compared it to the wild type MarR-PmarO system using gradient concentrations of SA (Figure 2d). The promoter S14 enabled an expanded dynamic range of the sensor system compared to the wild type PmarO promoter. Since the induced promoter S14 still cannot reach its maximum strength (PC), we also investigated whether the addition of SA would cause negative effect on protein expression. However, there was no obvious influence on the S14 promoter activity when gradient concentrations of SA were added (Supplementary Figure S2b). As this promoter can also be strictly inhibited by MarR, it could be a good option to be applied in SA related high-throughput screenings. Contrary to single-site hybrid promoters (S1~S5) that only showed very limited increases in activities after induced by SA, the dual-site hybrid promoters can not only be inhibited by MarR, but also can be activated by SA with better dynamic performance. These results confirmed our hypothesis that a secondary binding box is required for better releasing the MarR inhibition.

Site-directed mutagenesis on S14 promoter guided by modeling simulation

As the engineered S14-MarR biosensor system showed an extended dynamic range, we next sought to explore how the dynamic performance of the biosensor system can be tuned by further engineering the S14 promoter. We hypothesized that the strong binding between MarR protein and marO boxes hindered the release of MarR after induction by SA. To test this hypothesis, we first attempt to alleviate the interaction between MarR protein and the DNA sequences. To this end, a dynamic model was applied to simulate the binding process (see Methods for details). Using a program named visual molecular dynamics (VMD),[35] a computational model was generated in which the MarR-Binding sequence immersed in a water sphere mimicking the physiological environment (Figure 3a). Simulating this MarR-DNA complex in Nanoscale Molecular Dynamics (NAMD) revealed the binding frequency

and binding energy of every interaction between MarR residues and nucleotides (Figure 3b, Supplementary Table S1). Some nucleotides may bind to multiple residues on MarR protein and in this case the binding energy represented the sum of overall interactions. After the simulation, we found that the nucleotides 7G and 12G in binding box I and binding box II were predicted to possess the most and second highest binding frequencies and relatively high binding energies, which indicated that these two nucleotides played major roles in the binding between MarR and marO boxes. For the purpose of weakening the binding between MarR and the promoter, we mutated 7G and 12G to other nucleotides in the binding box I and II of S14 promoter. A total of twelve single-site mutants (I7G to A, C, and T, plus I12G to A, C, and T, in both binding boxes) were constructed by site-directed mutagenesis. Surprisingly, all promoter variants only enabled greatly lowered eGFP expression levels even without introducing the MarR (Figure 3c). The highest promoter activity was observed in variant I12A (1628±41 a.u.), which decreased by around 83% compared to the original S14 promoter (9662±1368 a.u.). After introducing the pCS27-lpp0.5-marR and inducing with SA, all promoter variants except for the I7T can be inhibited by MarR, but only the variant I12A exhibited improved activity when induced by 10 mM SA (Figure 3c). However, even though 65.29% activity of I12A can be recovered, the maximum promoter activity of I12A was only around 1600 a.u., making it unsuitable for applications in metabolic engineering. It was unclear why the mutation caused such hugely decreased promoter activities. Based on our results, the mutagenesis on these two critical nucleotides, though may weaken the binding between MarR and the promoter (as shown in variant I12A), cannot improve the dynamic range of the sensor system. Therefore, we next sought to mutate the nucleotides that possessed the third and fourth highest binding frequency and binding energy, which are the 4C and 5T in binding box I, plus 4C and 14C on binding box II (Figure 3b). Similar to the first-round mutagenesis, a total of twelve mutants were constructed, including the I4A, I4T, I4G, I5A, I5C, I5G, II4A, II4T, II4G, II14A, II14T, and II14G. Similar to the results of mutating 7G and 12G in the binding boxes, most of the promoters showed hugely decreased activities, except for the variant II4T (11573±558 a.u.) and II14T (8901±300 a.u.) (Figure 3d). These two variants maintained comparable maximum activities to the original S14 promoter (9662±1368 a.u.), and the II14T even showed a 19.78% increase in the maximum promoter activity. Further introduction of MarR (controlled by lpp0.5 in pCS plasmid) successfully resulted in inhibition on both promoters, though both the II4T and II14T showed prominent leaky activities (4724±44 and 2912±89 a.u., respectively). Upon the induction of 10 mM SA, the promoter activities of II4T and II14T were extended to 6411±73 a.u. and 5282±115 a.u. respectively, which represented a 3.89-fold and a 3.21-fold increase compared to the induced activity of S14 (1647±58 a.u.), respectively. These results indicated that these two promoters enabled more relaxed binding towards MarR, because they exhibited much higher induced activities compared to their parental promoter S14. This demonstrated that the dynamic performance of the sensor system can be tuned by manipulating the binding affinity between MarR and the promoter. Since these two promoters showed evident leaky expression, and an increased MarR expression level may reduce such leaky activity (Figure 1c), we tested whether the increased expression level of MarR can suppress the leaky expression (Supplementary Figure S3). To our surprise, the increased availability of MarR did not result in obvious changes in the dynamic performance of both promoters (Supplementary Figure S3). As the

I12A in the first-round mutation showed a decreased promoter activity but still maintain the SA biosensor phenotype, we hypothesized that the further introduction of the mutation in I12A promoter into the promoter II4T and II14T would possibly result in decreased leaky activities. Besides, we also want to see how the dynamic performance of the sensor system would be affected when the mutation in II4T and II14T is combined. Thus, three dual-mutated promoters, I12AII4T, I12AII14T, and II4TII14T, were constructed and tested. The promoter II4TII14T completely lost the function, with no fluorescence intensity can be observed when the eGFP was controlled by this promoter (Figure 3e). As for the I12AII4T and I12AII14T, both promoters were inhibited by MarR (when controlled by lpp0.5), and can exhibit increased promoter strengths when 10mM SA was introduced (Figure 3e). The leaky activities of the I12AII4T (4820±349 a.u.) and I12AII14T (3034±137 a.u.), however, did not show very obvious changes as we would anticipate compared to their corresponding parental promoters II4T (4724±44 a.u.) and II14T (2912±89 a.u.), respectively. However, the activities of I12AII4T (8833±152 a.u.) and I12AII14T (9061±472 a.u.) recovered by 10mM SA were boosted by 1.38-fold and 1.72-fold respectively, with around 84.43% and 79.95% of the maximum activities can be recovered respectively (Figure 3e). Finally, gradient concentrations of SA were added to determine the dynamic ranges of the sensor system when harboring the promoter I12AII4T and I12AII14T (Figure 3f). Compared with the wild type PmarO and S14, the promoter I12AII4T and I12AII14T showed increased sensitivities and positively shifted dynamic ranges (Figure 3f). This shift significantly improved the responsive strength of the promoter towards SA. In conclusion, guided by the dynamic modeling, the engineered promoters drastically improved the responsive strengths and shifted dynamic ranges of the MarR-PmarO biosensor system. These promoter variants will be beneficial for engineering SA-based dynamic pathway control or high-throughput screening of high producers for SA and its derived compounds.

Conclusion

Transcriptional factors-based biosensors (TFBs) are widely applied in metabolic engineering and synthetic biology. Nonetheless, natural TFBs often suffer from narrow dynamic ranges or low responsive activities. In this study, we systematically explored the tunability and engineering potentials of a natural MarR-PmarO biosensor system that can respond towards salicylic acid. We first investigated the effect of endogenous MarR on the dynamic performance of this sensor system. Besides, through fine-tuning the expression levels of MarR, we successfully improved the output strengths and dynamic ranges of this sensor system. Next, one of the regulatory elements, the marO binding box located in the PmarO promoter region, was demonstrated to be functional in a “plug-and-play” manner. By placing the marO binding boxes into the constitutive pL promoter, we obtained hybrid promoters that were responsive to MarR and SA with varied dynamic performance, which would be beneficial for future metabolic engineering. Last but not least, guided by the dynamic molecular modeling, we further explored the tunability of the sensor system by engineering the binding affinities between MarR and hybrid promoters. Finally, two representative variants, I12AII4T and I12AII14T, were obtained and demonstrated to have altered dynamic ranges, improved responsive strengths, and enhanced sensitivities. In summary, we demonstrated how a natural biosensor system with limited dynamic properties

can be engineered to have better performance. Our study will provide valuable insights for future engineering of natural transcriptional factors.

Methods & Materials

Strains & medium

Luria–Bertani (LB) medium was used for *E. coli* inoculation and plasmid propagation. If necessary, appropriate antibiotics including ampicillin and kanamycin were supplemented into the medium at the final concentration of 100 and 50 μg/mL, respectively. The *E. coli* strain XL1-Blue was used as the host strain for plasmid construction. Strain *E. coli* BW25113 (F') and its knockout derivatives *E. coli* BW25113 (F') *ΔmarR* were used in this research for dynamic performance test. *E. coli* BW25113 (F') *ΔmarR* were created via homologous recombination by replacing kanamycin on the original site of *marR* in genome. Salicylic Acid were purchased from Sigma-Aldrich.

DNA manipulation

Plasmids pZE12-luc (high-copy number) and pCS27 (medium-copy number) [30] were employed for constructing the biosensor system in this work (see Table 1 for a list of all strains and plasmids used in this study). For initial characterization of the MarR-PmarO biosnesor system, the PmarO promoter sequence was amplified from genomic DNA of *Escherichia coli* and used to replace the pLlacO1 promoter of pZE12-pLlacO1-eGFP [36] using XhoI and EcoRI to generate pZE12-PmarO-eGFP. To express MarR regulator in *Escherichia coli*, we substituted the eGFP gene to MarR in pCS27-lpp-eGFP using Acc65I and BamHI, resulting in the pCS27-lpp-MarR.

For construction of hybrid promoters, a parental plasmid pZE12-pL-eGFP was generated from pZE12-pLlacO1-eGFP by replacing the pLlacO1 promoter with the pL promoter sequence [37]. We selected five sites (site 1~5, Figure 2a) on pL promoter to substitute MarO binding boxes. For the site 1 (from −60bp to −37bp), site 3 (−33bp to −13bp), and site 5 (−7bp to +16bp), the sequences of the binding boxes were used to directly replacing the original pL promoter sequences. For site 2 or site 4 that overlaps with the −35 or −10 region respectively, the binding boxes were split to two sections and the original −35 and −10 sequences from pL promoter were reserved. In doing so, we want to avoid the disruption of the −10 and −35 region. Thus, in site 2, the sequences from −46bp to −36bp and from −30bp to −17bp were replaced by the sequences from the marO binding boxes, and in site 4, the sequences from −27bp to −17bp, and −11bp to −1bp, were replaced by sequences from binding boxes. The DNA sequences for all hybrid promoters were listed in Table 2.

Cultivation conditions

All transformants were cultured in 3.5 mL LB medium with appropriate antibiotics at 37 °C with a shaking speed at 270 rpm in the New Brunswick Excella E24 shaker (orbital diameter: 19.1mm). 150μL cultures were transferred into test tubes containing fresh 3.5mL LB medium with appropriate antibiotics. The cells were then cultivated at 37 °C with a shaking speed at 270 rpm. Different concentrations of salicylic acid (SA) in sodium salt form were added into medium after 1.5 h (when OD_{600} reached approximately 0.4). Before

feeding, the pH of the SA stock in sodium salt form was adjusted to 7.0 to eliminate the potential negative effects of pH-related toxicity on cell growth and protein expression. The samples were collected at appropriate time point and then subjected to measurement of cell densities (OD_{600}) and green fluorescence intensities.

Fluorescence Assays

The Synergy HT plate reader from Biotek was used for fluorescence assays. The samples were diluted by 5 times (40 μL sample with 160 μL water) and transferred into a black 96-well plate with clear bottom (Corning 3603). The plate was scanned in the Synergy HT (BioTek) plate reader. The eGFP fluorescence intensity was detected by using an excitation filter of 485/20 nm and an emission filter of 528/20 nm The cell densities (OD_{600}) were also collected using this plate reader.

MarR-DNA dynamic model simulation

The software Visual Molecular Dynamics (VMD) [35] was applied to construct the simulation model of the MarR-DNA-water complex. The three-dimensional structure of the MarR protein was obtained from the pdb file indexed “5h3r” [38] from the RCSB protein data bank. Meanwhile, two binding boxes were imported to the model separately to form two MarR-DNA complexes with different DNA sequences. The MarR-DNA complex was immersed into a water sphere in order to closely resemble the cellular environment. Note that it is not necessary to make the shape of water droplet spherical. Nevertheless, energy minimization and equilibration will deform the water droplet into the most stable shape with a minimal surface tension, namely sphere. For simplicity, we did not add ions, like Na^+, K^+, Cl^- into simulation surroundings. Here, we considered covalent bonding, van der Waals forces, and electrostatic interactions into the binding energy between MarR residues and each nucleotide. To well describe the interactions among atoms in the MarR-DNA-water complex, CHARMM36 [39] force field was adopted. The potential form of the force field is given as follows:

$$E = E_{bond} + E_{angle} + E_{dihedral} + E_{impropers} + E_{Urey-Bradley} + E_{vdW} + E_{elec}, \quad (1)$$

where the first five terms account for the short-range covalent bonding interactions while the last two terms are associated with long-range van der Waals and electrostatic forces. The cutoff distance for van der Waals and electrostatic interactions was set to be 12 Å.

The software Nanoscale Molecular Dynamics (NAMD) [40] was used to simulate the binding process of established MarR-DNA complexes. The environmental temperature was set at 310 K and the timestep was set at 2 femtoseconds. Two MarR-DNA complexes were introduced into NAMD. The simulation ran for 4ns until the potential energy change of the complexes is marginal (<5% of the binding energy). After this process, a series of binding frequencies between each nucleotide and residues were obtained. Considering the primary molecular forces, binding energy on each nucleotide could be calculated by summing up covalent bonding, van der Waals forces, and electrostatic interactions.

Supplementary Material

Refer to Web version on PubMed Central for supplementary material.

Acknowledgement

This work was supported by the National Institute of General Medical Sciences of the National Institutes of Health under award number R35GM128620. We also acknowledge the support from the College of Engineering, The University of Georgia, Athens.

References:

1. Woolston BM; Edgar S; Stephanopoulos G, Metabolic engineering: past and future. Annu Rev Chem Biomol Eng 2013, 4, 259–88. [PubMed: 23540289]
2. Zhang J; Jensen MK; Keasling JD, Development of biosensors and their application in metabolic engineering. Curr Opin Chem Biol 2015, 28, 1–8. [PubMed: 26056948]
3. Shen X; Wang J; Li C; Yuan Q; Yan Y, Dynamic gene expression engineering as a tool in pathway engineering. Curr Opin Biotechnol 2019, 59, 122–129. [PubMed: 31063878]
4. Zhang R; Li C; Wang J; Yan Y, Microbial Ligninolysis: Toward a Bottom-Up Approach for Lignin Upgrading. Biochemistry 2019, 58 (11), 1501–1510. [PubMed: 30351915]
5. Huo YX; Cho KM; Rivera JG; Monte E; Shen CR; Yan Y; Liao JC, Conversion of proteins into biofuels by engineering nitrogen flux. Nat Biotechnol 2011, 29 (4), 346–51. [PubMed: 21378968]
6. Zhang R; Li C; Wang J; Yang Y; Yan Y, Microbial production of small medicinal molecules and biologics: From nature to synthetic pathways. Biotechnol Adv 2018, 36 (8), 2219–2231. [PubMed: 30385278]
7. Shen X; Wang J; Wang J; Chen Z; Yuan Q; Yan Y, High-level De novo biosynthesis of arbutin in engineered Escherichia coli. Metab Eng 2017, 42, 52–58. [PubMed: 28583673]
8. Wang J; Li C; Zou Y; Yan Y, Bacterial synthesis of C3-C5 diols via extending amino acid catabolism. Proc. Natl. Acad. Sci. U. S. A 2020, 117 (32), 19159–19167. [PubMed: 32719126]
9. Mahr R; Frunzke J, Transcription factor-based biosensors in biotechnology: current state and future prospects. Appl Microbiol Biotechnol 2016, 100 (1), 79–90. [PubMed: 26521244]
10. Emmerstorfer-Augustin A; Moser S; Pichler H, Screening for improved isoprenoid biosynthesis in microorganisms. J Biotechnol 2016, 235, 112–20. [PubMed: 27046070]
11. Eggeling L; Bott M; Marienhagen J, Novel screening methods--biosensors. Curr Opin Biotechnol 2015, 35, 30–6. [PubMed: 25578902]
12. Tan SZ; Prather KL, Dynamic pathway regulation: recent advances and methods of construction. Curr Opin Chem Biol 2017, 41, 28–35. [PubMed: 29059607]
13. Tang SY; Cirino PC, Design and application of a mevalonate-responsive regulatory protein. Angew Chem Int Ed Engl 2011, 50 (5), 1084–6. [PubMed: 21268200]
14. Stephan Binder GS, Norma Stäbler, Karin Krumbach, Kristina Hoffmann, Michael Bott and Lothar Eggeling*, A high-throughput approach to identify genomic variants of bacterial metabolite producers at the single-cell level. Genome Biol 2012, 13.
15. Tang SY; Qian S; Akinterinwa O; Frei CS; Gredell JA; Cirino PC, Screening for enhanced triacetic acid lactone production by recombinant Escherichia coli expressing a designed triacetic acid lactone reporter. J Am Chem Soc 2013, 135 (27), 10099–103. [PubMed: 23786422]
16. Liao JC, a. F. WR, Improving lycopene production in Escherichia coli by engineering metabolic control. NATURE BIOTECHNOLOGY 2000, 18.
17. Doong SJ; Gupta A; Prather KLJ, Layered dynamic regulation for improving metabolic pathway productivity in Escherichia coli. Proc Natl Acad Sci U S A 2018, 115 (12), 2964–2969. [PubMed: 29507236]
18. Zhang F; Carothers JM; Keasling JD, Design of a dynamic sensor-regulator system for production of chemicals and fuels derived from fatty acids. Nat Biotechnol 2012, 30 (4), 354–9. [PubMed: 22446695]

19. Zhang F; Ouellet M; Batth TS; Adams PD; Petzold CJ; Mukhopadhyay A; Keasling JD, Enhancing fatty acid production by the expression of the regulatory transcription factor FadR. Metab Eng 2012, 14 (6), 653–60. [PubMed: 23026122]

20. Yang Y; Lin Y; Wang J; Wu Y; Zhang R; Cheng M; Shen X; Wang J; Chen Z; Li C; Yuan Q; Yan Y, Sensor-regulator and RNAi based bifunctional dynamic control network for engineered microbial synthesis. Nat Commun 2018, 9 (1), 3043. [PubMed: 30072730]

21. Cohen SP; Hachler H; Levy SB, Genetic and functional analysis of the multiple antibiotic resistance (mar) locus in Escherichia coli. Journal of Bacteriology 1993, 175, 1484–1492. [PubMed: 8383113]

22. COHEN SETHP, L. SB, FOULDS JOHN, AND ROSNER JUDAHL, Salicylate Induction of Antibiotic Resistance in Escherichia coli: Activation of the mar Operon and a mar-Independent Pathway. JOURNAL OF BACTERIOLOGY 1993, 7856–7862. [PubMed: 7504664]

23. LEVY MNAASB, Alteration of the Repressor Activity of MarR, the Negative Regulator of the Escherichia coli marRAB Locus, by Multiple Chemicals In Vitro. JOURNAL OF BACTERIOLOGY 1999, 4669–4672. [PubMed: 10419969]

24. Alekshun Michael N., L. SB, Mealy Tanya R., Seaton Barbara A. and Head James F., The crystal structure of MarR, a regulator of multiple antibiotic resistance, at 2.3 Å resolution. Nature structural biology 2001, 8, 710–714. [PubMed: 11473263]

25. Alekshun Michael N., K. YS a. L. SB, Mutational analysis of MarR, the negative regulator of marRAB expression in Escherichia coli, suggests the presence of two regions required for DNA binding. Molecular Microbiology 2000, 35(6), 1394–1404. [PubMed: 10760140]

26. Hao Z; Lou H; Zhu R; Zhu J; Zhang D; Zhao BS; Zeng S; Chen X; Chan J; He C; Chen PR, The multiple antibiotic resistance regulator MarR is a copper sensor in Escherichia coli. Nat Chem Biol 2014, 10 (1), 21–8. [PubMed: 24185215]

27. Shen CR; Liao JC, Metabolic engineering of Escherichia coli for 1-butanol and 1-propanol production via the keto-acid pathways. Metab Eng 2008, 10 (6), 312–20. [PubMed: 18775501]

28. Wang J; Mahajani M; Jackson SL; Yang Y; Chen M; Ferreira EM; Lin Y; Yan Y. J. M. e., Engineering a bacterial platform for total biosynthesis of caffeic acid derived phenethyl esters and amides. 2017, 44, 89–99.

29. Lutz R; Bujard H. J. N. a. r., Independent and tight regulation of transcriptional units in Escherichia coli via the LacR/O, the TetR/O and AraC/I1-I2 regulatory elements. 1997, 25 (6), 1203–1210.

30. Jiang T; Li C; Yan Y, Optimization of a p-Coumaric Acid Biosensor System for Versatile Dynamic Performance. ACS Synth Biol 2021, 10 (1), 132–144. [PubMed: 33378169]

31. Martin RG; Rosner JL, Transcriptional and translational regulation of the marRAB multiple antibiotic resistance operon in Escherichia coli. Mol Microbiol 2004, 53 (1), 183–91. [PubMed: 15225313]

32. Cox RS III; Surette MG; Elowitz MB, Programming gene expression with combinatorial promoters. Molecular Systems Biology 2007, 3 (1), 145. [PubMed: 18004278]

33. Egland KA; Greenberg E, Quorum sensing in Vibrio fischeri: elements of the luxI promoter. Molecular microbiology 1999, 31 (4), 1197–1204. [PubMed: 10096086]

34. Collado-Vides J; Magasanik B; Gralla JD, Control site location and transcriptional regulation in Escherichia coli. Microbiological reviews 1991, 55 (3), 371–394. [PubMed: 1943993]

35. Humphrey W; Dalke A; Schulten K, VMD: Visual molecular dynamics. Journal of Molecular Graphics 1996, 14 (1), 33–38. [PubMed: 8744570]

36. Yang Y; Lin Y; Li L; Linhardt RJ; Yan Y. J. M. e., Regulating malonyl-CoA metabolism via synthetic antisense RNAs for enhanced biosynthesis of natural products. 2015, 29, 217–226.

37. Bernard H-U; Remaut E; Hershfield MV; Das HK; Helinski DR; Yanofsky C; Franklin NJG, Construction of plasmid cloning vehicles that promote gene expression from the bacteriophage lambda pL promoter. 1979, 5(1), 59–76.

38. Zhu R; Hao Z; Lou H; Song Y; Zhao J; Chen Y; Zhu J; Chen PR, Structural characterization of the DNA-binding mechanism underlying the copper(II)-sensing MarR transcriptional regulator. JBIC Journal of Biological Inorganic Chemistry 2017, 22 (5), 685–693. [PubMed: 28124121]

39. Best RB; Zhu X; Shim J; Lopes PEM; Mittal J; Feig M; MacKerell AD, Optimization of the Additive CHARMM All-Atom Protein Force Field Targeting Improved Sampling of the Backbone

ϕ, ψ and Side-Chain χ1 and χ2 Dihedral Angles. Journal of Chemical Theory and Computation 2012, 8 (9), 3257–3273. [PubMed: 23341755]

40. Nelson MT; Humphrey W; Gursoy A; Dalke A; Kalé LV; Skeel RD; Schulten K, NAMD: a Parallel, Object-Oriented Molecular Dynamics Program. The International Journal of Supercomputer Applications and High Performance Computing 1996,10 (4), 251–268.

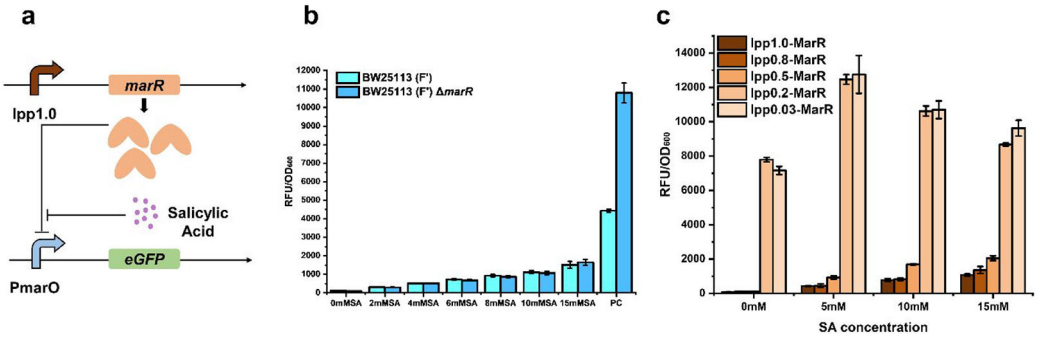

Figure 1. Establishment and validation of MarR-PmarO biosensor system.

a) Schematic graph of re-established MarR-PmarO biosensor system. MarR protein binds on PmarO to inhibit promoter expression and SA binds with MarR protein to release the repression. b) Dynamic performance of wild type MarR-PmarO biosensor system in wild type *E. coli* BW25113(F′) and *E. coli* Δ*marR*. PC, positive control, which represents PmarO promoter strength without exogenous MarR. c) Fine-tuning of MarR-PmarO biosensor system by lpp promoter variants. The strain *E. coli* Δ*marR* was used in this test. The data were obtained after 24 hours cultivation in test tubes. Error bars represent standard deviation (n=3).

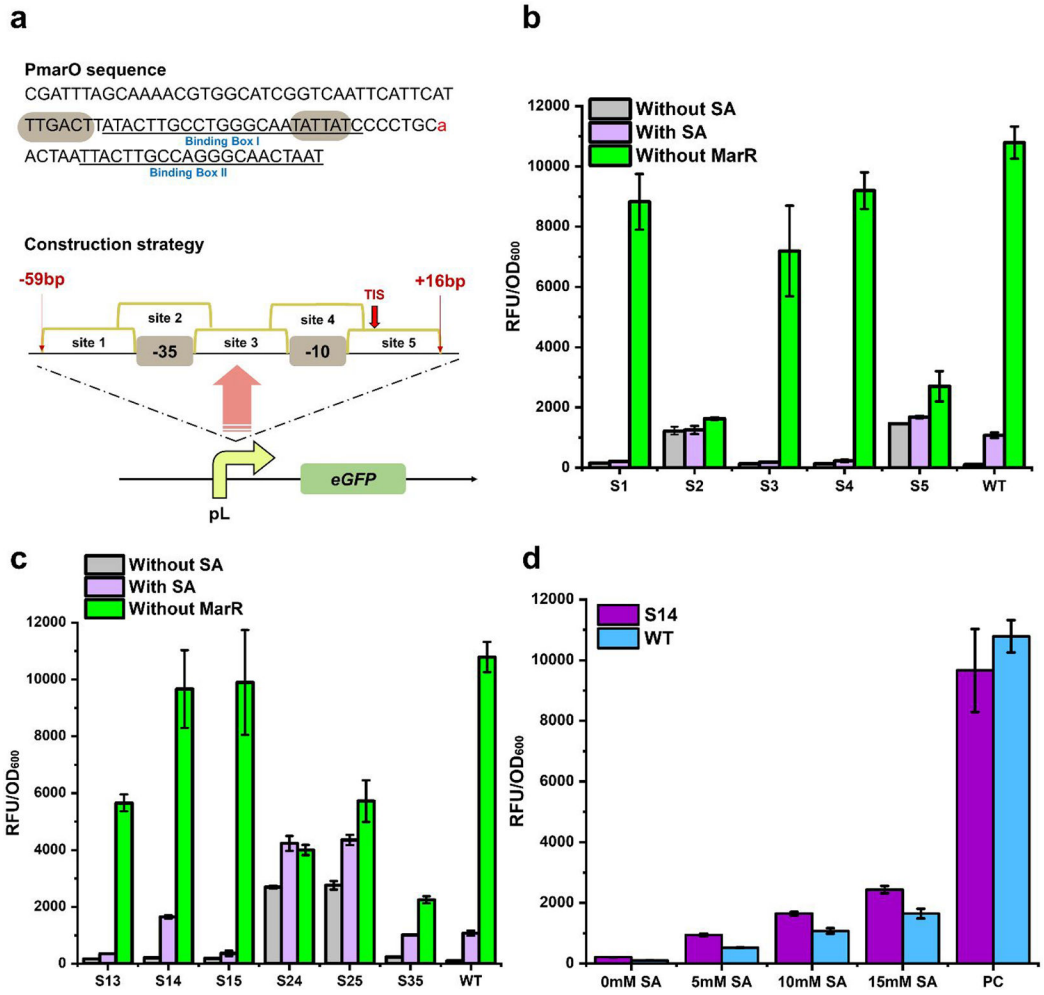

Figure 2. Construction strategy and dynamic performance of hybrid promoters

a) Promoter sequence of PmarO and construction strategy of hybrid promoters. The highlighted regions in the PmarO promoter sequence represent the −35 and −10 boxes. TIS, transcription initial site, which is the letter in red. b) Dynamic performance of one-site hybrid promoters. WT, wild type PmarO promoter. c) Dynamic performance of dual-site hybrid promoters. WT, wild type MarR-PmarO biosensor system. d) Dynamic ranges of the sensor system enabled by S14 and WT PmarO promoter. PC, positive control, which represents promoter activity without MarR. Error bars represent standard deviation (n=3).

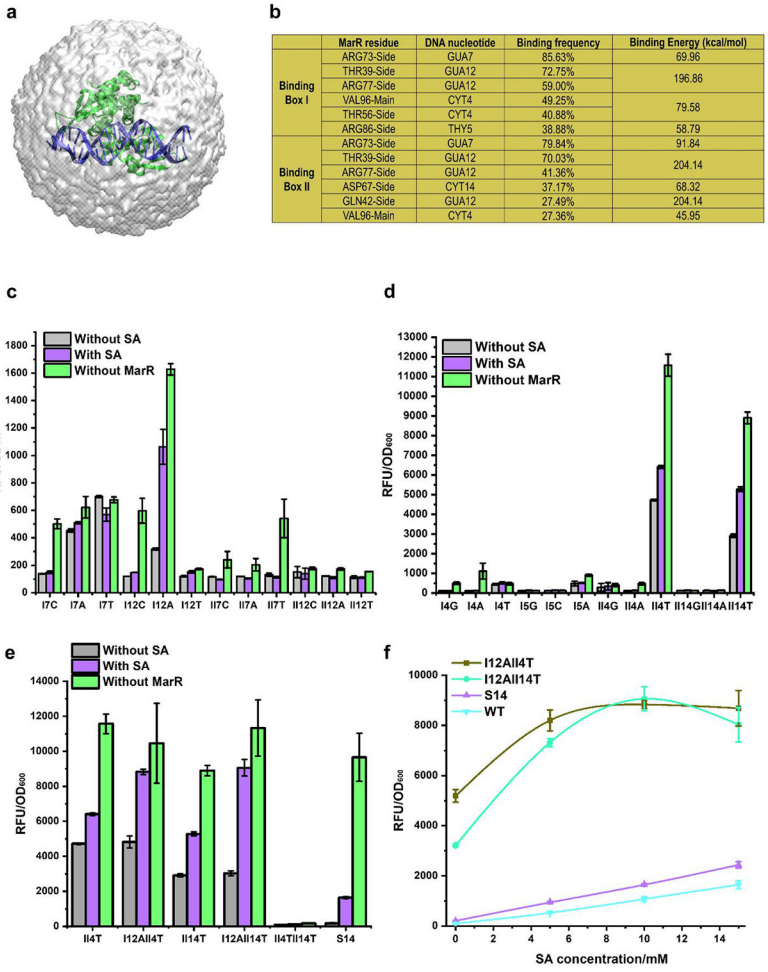

	MarR residue	DNA nucleotide	Binding frequency	Binding Energy (kcal/mol)
Binding Box I	ARG73-Side	GUA7	85.63%	69.96
	THR39-Side	GUA12	72.75%	196.86
	ARG77-Side	GUA12	59.00%	
	VAL96-Main	CYT4	49.25%	79.58
	THR56-Side	CYT4	40.88%	
	ARG86-Side	THY5	38.88%	58.79
Binding Box II	ARG73-Side	GUA7	79.84%	91.84
	THR39-Side	GUA12	70.03%	204.14
	ARG77-Side	GUA12	41.36%	
	ASP67-Side	CYT14	37.17%	68.32
	GLN42-Side	GUA12	27.49%	204.14
	VAL96-Main	CYT4	27.36%	45.95

Figure 3. Dynamic modeling simulation results and dynamic performance of promoter variants

a) Scheme of modeling simulation. A water sphere structure including MarR protein and identified DNA sequence was built in VMD. MarR protein was drew in green color and DNA sequence of binding boxes was drew in purple color. b) Binding frequencies and binding energies of dominant nucleotides. Binding frequency and binding energy were calculated by NAMD. c) Dynamic performance of 12 promoter variants from first-round mutagenesis. Green column represented strength of mutated promoters without regulator protein. WT, wild type MarR-PmarO biosensor system. d) Dynamic performance of 12 promoter variants from the second-round mutagenesis. e) Dynamic performance of three promoters with double mutations and their parental promoters. f) Dynamic ranges of sensor systems enabled by promoter WT PmarO, S14, I12AII4T, and I12AII14T. Error bars represent standard deviation (n=3).

Table 1.

Strains and Plasmids used in this study

Strain	**Genotype**	**Reference**
E. coli XL1-Blue	*recA1 endA1gyrA96thi-1hsdR17supE44relA1lac[F´ proAB lacIqZDM15Tn10 (TetR)] rrnBT14 ΔlacZWJ16 hsdR514 ΔaraBADAH33*	Stratagene
E. coli BW25113(F')	*ΔrhaBADLD78 F´ [traD36 proAB lacIqZΔM15 Tn10(Tetr)]*	[20]
E. coli BW25113 (F') Δ*marR*	*E. coli* BW25113 (F') *marR*:kanR	This study
Plasmid	**Description**	**Reference**
pZE12-luc	P_{LlacO1} colE ori, luc, Amp^r	[29]
pCS27	P_{LlacO1}, P15A ori, Kan^r	[27]
pZE12-pLlacO1-eGFP	pZE12 with eGFP under the control of P_{LlacO1}	[30]
pZE12-PmarO-eGFP	pZE12 with eGFP under the control of PmarO	This study
pZE12-pL-eGFP	pZE12 with eGFP under the control of pL	This study
pZE12-S1-eGFP	pZE12 with eGFP under the control of promoter S1	This study
pZE12-S2-eGFP	pZE12 with eGFP under the control of promoter S2	This study
pZE12-S3-eGFP	pZE12 with eGFP under the control of promoter S3	This study
pZE12-S4-eGFP	pZE12 with eGFP under the control of promoter S4	This study
pZE12-S5-eGFP	pZE12 with eGFP under the control of promoter S5	This study
pZE12-S13-eGFP	pZE12 with eGFP under the control of promoter S13	This study
pZE12-S14-eGFP	pZE12 with eGFP under the control of promoter S14	This study
pZE12-S15-eGFP	pZE12 with eGFP under the control of promoter S15	This study
pZE12-S24-eGFP	pZE12 with eGFP under the control of promoter S24	This study
pZE12-S25-eGFP	pZE12 with eGFP under the control of promoter S25	This study
pZE12-S35-eGFP	pZE12 with eGFP under the control of promoter S35	This study
pCS27-lpp1.0-eGFP	pCS27 with eGFP under the control of promoter lpp1.0	[28]
pCS27-lpp1.0-MarR	pCS27 with MarR under the control of promoter lpp1.0	This study
pCS27-lpp0.8-MarR	pCS27 with MarR under the control of promoter lpp0.8	This study
pCS27-lpp0.5-MarR	pCS27 with MarR under the control of promoter lpp0.5	This study
pCS27-lpp0.2-MarR	pCS27 with MarR under the control of promoter lpp0.2	This study
pCS27-lpp0.03-MarR	pCS27 with MarR under the control of promoter lpp0.03	This study

Table 2.

Gene sequences used in this study

Name	Sequence
MarR	GTGAAAAGTACCAGCGATCTGTTCAATGAAATTATTCCATTGGGTCGCTTAATCCAT ATGGTTAATCAGAAGAAAGATCGCCTGCTTAACGAGTATCTGTCTCCGCTGGATATT ACCGCGGCACAGTTTAAGGTGCTCTGCTCTATCCGCTGCGCGGCGTGTATTACTCCG GTTGAACTGAAAAAGGTATTGTCGGTCGACCTGGGAGCACTGACCCGTATGCTGGA TCGCCTGGTCTGTAAAGGCTGGGTGGAAAGGTTGCCGAACCCGAATGACAAGCGCG GCGTACTGGTAAAACTTACCACCGGCGGCGCGGCAATATGTGAACAATGCCATCAA TTAGTTGGCCAGGACCTGCACCAAGAATTAACAAAAAACCTGACGGCGGACGAAGT GGCAACACTTGAGTATTTGCTTAAGAAAGTCCTGCCGTAA
PmarO	CGATTTAGCAAAACGTGGCATCGGTCAATTCATTCATTTGACTTATACTTGCCTGGG CAATATTATCCCCTGCAACTAATTACTTGCCAGGGCAACTAAT
pL	TAAATTATCTCTGGCGGTGTTGACATAAATACCACTGGCGGTGATACTGAGCACATC AGCAGGACGCACTGACC
S1	ATACTTGCCTGGGCAATATTATCTTGACATAAATACCACTGGCGGTGATACTGAGCA CATCAGCAGGACGCACTGACC
S2	TAAATTATCATACTTGCCTTTGACAGGGCAATATTATCCGGTGATACTGAGCACATC AGCAGGACGCACTGACC
S3	TAAATTATCTCTGGCGGTGTTGACACTTGCCTGGGCAATATTGATACTGAGCACATC AGCAGGACGCACTGACC
S4	TAAATTATCTCTGGCGGTGTTGACATAAATACATACTTGCCTGATACTGGGCAATAT TATCTCAGCAGGACGCACTGACC
S5	TAAATTATCTCTGGCGGTGTTGACATAAATACCACTGGCGGTGATACTATACTTGCC TGGGCAATATTATCACC
S13	ATACTTGCCTGGGCAATATTATCTTGACATTACTTGCCAGGGCAACTAATGATACTG AGCACATCAGCAGGACGCACTGACC
S14	ATACTTGCCTGGGCAATATTATCTTGACATAAATACTTACTTGCCAGATACTGGGCA ACTAATTCAGCAGGACGCACTGACC
S15	ATACTTGCCTGGGCAATATTATCTTGACATAAATACCACTGGCGGTGATACTTTACT TGCCAGGGCAACTAATTCAGCAGGACGCACTGACC
S24	TAAATTATCATACTTGCCTTTGACAGGGCAATATTATCTTACGATACTTTGCCAGGG CAACTAATTCAGCAGGACGCACTGACC
S25	TAAATTATCATACTTGCCTTTGACAGGGCAATATTATCCGGTGATACTTTACTTGCCA GGGCAACTAATTCAGCAGGACGCACTGACC
S35	TAAATTATCTCTGGCGGTGTTGACAATACTTGCCTGGGCAATATTATCGATACTTTAC TTGCCAGGGCAACTAATTCAGCAGGACGCACTGACC